Formate Ester Norrish Type II Elimination: Diode Laser Probing of Gas-Phase Yields

Yuping Niu, Elizabeth Christophy, Patrick J. Pisano, Ying Zhang, and Jeanne M. Hossenlopp*

Contribution from the Department of Chemistry, Marquette University, P.O. Box 1881, Milwaukee, Wisconsin 53201-1881

Received July 28, 1995[⊗]

Abstract: Time-resolved infrared absorption spectroscopy was utilized to monitor the production of HCOOH, CO_2, and CO following ultraviolet laser excitation of gas-phase formate esters. Excitation of ethyl formate at 227.5 nm resulted in formation of HCOOH and CO_2. The CO_2 quantum yield was estimated to be 0.5 ± 0.1. No evidence for CO formation was obtained at this wavelength. Relative quantum yields for the Norrish Type II elimination of HCOOH from ethyl, *n*-propyl, *n*-butyl, isopropyl, isobutyl, and *tert*-butyl formate were obtained at 227.5 and 222 nm. Normalization of the observed HCOOH yields with respect to the number of γ-hydrogen atoms resulted in reactivity trends at 227.5 nm of 1:3:9 for the abstraction of primary, secondary, and tertiary hydrogen atoms, respectively. At 222 nm, a similar reactivity trend was observed with yields per available γ-hydrogen of 1:3:7 for abstraction of primary, secondary, and tertiary hydrogen atoms. Yields were found to be independent of ester pressure over the range 100−550 mTorr. Semiempirical and *ab initio* calculations of the excited state hydrogen abstraction step were performed and enthalpies of activation of 8−12 kcal/mol were obtained using AM1 with configuration interaction.

Introduction

Excitation of the A ← X transition in moderate-sized aliphatic carbonyl compounds results in competing photochemical channels. Following excitation of the weak $^1(n\pi^*)$ chromophore, a complex array of photoproducts may be observed.[1] The primary channels observed when the initial carbonyl has hydrogen atoms at the γ-position relative to the carbonyl group are the Norrish Type I cleavage of one of the bonds adjacent to the carbonyl group and the Norrish Type II and Yang reactions initiated by intramolecular hydrogen atom abstraction. For a variety of small-to-moderate size carbonyl compounds, insight into the nature of the potential energy surfaces involved in the Norrish Type I bond cleavage channels has been obtained from gas-phase studies of the product energy distributions.[2]

The basic photochemistry of the Norrish Type II reaction has been extensively reviewed.[3] There is also an increasing number of theoretical investigations.[4−7] In addition to its fundamental importance as an example of the general class of intramolecular hydrogen abstraction reactions and its common occurrence in carbonyl photochemistry, the Norrish Type II reaction has found applications such as the synthesis of enediynes.[8] Understanding the factors which control product branching ratios is of particular importance for this class of photoinduced reaction. Investigation of product yields in constrained media[9] such as liquid crystals and zeolites has been used to highlight the role of internal rotation to the appropriate transition states for both the hydrogen abstraction step and the elimination from the diradical intermediate.

Direct, *in-situ* detection of gas-phase Norrish Type II products would provide additional insight into this reaction by minimizing, or even eliminating, the influence of reaction medium. While there have been examples of gas-phase studies,[10] the capabilities of high-resolution spectroscopic probing of reaction products have not been exploited for this reaction. The focus of our work is the exploration of molecular structure effects on photochemical kinetics and dynamics. One objective is to determine the role of reactant structure in influencing yields of Norrish Type II elimination products obtained in the gas phase. The second objective is to provide a new view of these reactions by investigating their dynamics via characterization of quantum-state-resolved energy distributions of the products.

The subject of the work reported here is an investigation of the Norrish Type II elimination from a series of alkyl formate esters. Time-resolved infrared diode laser spectroscopy was used to probe the yields of HCOOH from six formate esters in order to investigate molecular structure effects on this process. Semiempirical and *ab initio* calculations of the hydrogen

[⊗] Abstract published in *Advance ACS Abstracts,* April 15, 1996.

(1) Calvert, J. G.; Pitts, J. N., Jr. *Photochemistry*; Wiley: New York, 1966.

(2) See, for example: (a) Woodbridge, E. L.; Fletcher, T. R.; Leone, S. R. *J. Phys. Chem.* **1988**, *92*, 5387. (b) Brouard, M.; O'Mahony, J. *Chem. Phys. Lett.* **1988**, *149*, 45. (c) Ebata, T.; Amano, T.; Ito, M. *J. Chem. Phys.* **1989**, *90*, 112. (d) Trentelman, K. A.; Kable, S. H.; Moss, D. B.; Houston, P. L. *J. Chem. Phys.* **1989**, *91*, 7498. (e) Hunnicutt, S. S.; Waits, L. D.; Guest, J. A. *J. Phys. Chem.* **1991**, *95*, 562. (f) Person, M. D.; Kash, P. W.; Butler, L. J. *J. Phys. Chem.* **1992**, *96*, 2021. (g) North, S. W.; Blank, D. A.; Gezelter, J. D.; Longfellow, C. A.; Lee, Y. T. *J. Chem. Phys.* **1994**, *102*, 4447. (h) Gejo, T.; Takayanagi, M.; Koro, T.; Hanazaki, I. *Chem. Phys. Lett.* **1994**, *218*, 343. (i) Terentis, A. C.; Stone, M.; Kable, S. H. *J. Phys. Chem.* **1994**, *98*, 10802. (j) Hall, G. E.; Metzler, H. W.; Muckermann, J. T.; Preses, J. M.; Weston, R. E., Jr. *J. Chem. Phys.* **1995**, *102*, 6660.

(3) (a) Wagner, P. J. *Acc. Chem. Res.* **1971**, *4*, 168. (b) Scaiano, J. C.; Lissi, E. A.; Encina, M. V. *Rev. Chem. Intermed.* **1978**, *2*, 139. (c) Wagner, P.; Park, B.-S. In *Organic Photochemistry*; Padwa, A., Ed.; Marcel Dekker: New York, 1991; Vol. 11, Chapter 4.

(4) Dewar, M. J. S.; Doubleday, C. *J. Am. Chem. Soc.* **1978**, *100*, 4935.

(5) Sengupta, D.; Sumathi, R.; Chandra, A. K. *J. Photochem. Photobiol. A: Chem.* **1991**, *60*, 149.

(6) Dorigo, A. E.; McCarrick, M. A.; Loncharich, R. J. *J. Am. Chem. Soc.* **1990**, *112*, 7508.

(7) Sauers, R. R.; Edberg, L. A. *J. Org. Chem.* **1994**, *59*, 7061.

(8) Nuss, J. M.; Murphy, M. M. *Tetrahedron Lett.* **1994**, *35*, 37.

(9) (a) Ramamurthy, V.; Corbin, D. R.; Eaton, D. F. *J. Org. Chem.* **1990**, *55*, 5269. (b) Ramamurthy, V.; Sanderson, D. R. *Tetrahedron Lett.* **1992**, *33*, 2757. (c) Ramamurthy, V.; Lei, X.-G.; Turro, N. J.; Lewis, T. J.; Scheffer, J. R. *Tetrahedron Lett.* **1991**, *32*, 7675. (d) Furman, I.; Butcher, R. J.; Catchings, R. M.; Weiss, R. G. *J. Am. Chem. Soc.* **1992**, *114*, 6023.

(10) For example: (a) Wettack, F. S.; Noyes, W. A., Jr. *J. Am. Chem. Soc.* **1968**, *90*, 3901. (b) Nicol, C. H.; Calvert, J. G. *J. Am. Chem. Soc.* **1967**, *89*, 1790.

S0002-7863(95)02532-7 CCC: $12.00

abstraction step were performed for comparison with observed trends in HCOOH production. The competition between the Norrish Type I channel which results in CO_2 formation and the Norrish Type II elimination was also explored.

Most of the previous experimental and theoretical work on Norrish Type II processes has been done on ketone or aldehyde reactants. Choice of these reactants would present an additional difficulty in the study of the reaction dynamics due to the enol−keto isomerization step. Production of an acid from the photolysis of esters eliminates this complication. Formate esters represent the simplest system of this type and there is well-documented[11] HCOOH rovibrational spectroscopy, making this the most attractive class of precursors for gas-phase photodissociation dynamics studies.

The onset of absorption for the $^1(n\pi^*)$ transition of formate esters is observed at 255 nm and the absorption peaks at approximately 215 nm.[1] Ethyl formate is the smallest ester which can undergo the Norrish Type II elimination. Review of the early photochemical studies on formate esters led to postulation[1] of four potentially important photodissociation channels as shown below for ethyl formate.

$$CH_3CH_2OCHO + h\nu \rightarrow CH_3CH_2O + HCO \quad (1)$$

$$\rightarrow CH_3CH_2CO_2 + H \quad (2)$$

$$\rightarrow CH_3CH_2OH + CO \quad (3)$$

$$\rightarrow CH_2CH_2 + HCOOH \quad (4)$$

Channels 1 and 2 are the Norrish Type I cleavage reactions. Facile thermal decarboxylation[12] from the alkoxyl product of channel 2 should result in CO_2 production. Carbon monoxide production has been reported for the photolysis of a variety of formate esters.[13,14] The Norrish Type II reaction is channel 4 above.

Preliminary survey work was performed to look for stable molecular productions from ethyl formate channels 2 through 4. Relative HCOOH yields were determined at 227.5 and 222 nm from methyl, ethyl, *n*-propyl, *n*-butyl, isopropyl, isobutyl, and *tert*-butyl formate. The basic experimental scheme is shown below for detection of HCOOH, CO_2, and CO using infrared diode laser absorption spectroscopy. HCOOH was monitored via the ν_3 carbonyl stretching mode. The rotational states of this asymmetric rotor are designated by $J_{Ka,Kc}$.

$$HCOOH(\nu_3 = 0, J''_{Ka'',Kc''}) + h\nu(\sim 1770\ cm^{-1}) \rightarrow HCOOH(\nu_3 = 1, J'_{Ka',Kc'}) \quad (5)$$

Use of the diode laser technique to monitor CO_2 and CO has been well-documented.[15] CO_2 was monitored via the antisymmetric stretching transition. The bending state, ν_2, quanta are designated as m^l and, in the work reported here, the probe transitions always involved lower states with no quanta of ν_1 symmetric stretch or ν_3 antisymmetric stretch excitation.

$$CO_2\ (0m^10, J) + h\nu\ (\sim 2270\ cm^{-1}) \rightarrow CO_2\ (0m^11, J \pm 1) \quad (6)$$

Carbon monoxide was also probed as shown below.

$$CO(\nu = 0, J) + h\nu\ (\sim 2100\ cm^{-1}) \rightarrow CO(\nu = 1, J \pm 1) \quad (7)$$

Experimental Section

Formic acid relative yield determinations were performed at 227.5 and 222 nm. For the 227.5-nm experiments, a Questek 2520 v-β XeCl excimer laser, operated at 1 Hz, was used to pump a Lambda Physik Fl3002 dye laser set at 445 nm. A dye solution of Coumarin 440 in methanol with DABCO added for dye stability was used. The output of the dye laser was directed through a BBO (B cut) crystal housed in an InRad autotracker. The doubled output was separated from the residual fundamental using a four-prism beam separator. Choice of this wavelength was made to maximize the UV output from our apparatus at a wavelength where the esters absorb. Upgrading the excimer laser to model 2720 enabled operation at 222 nm (KrCl).

Absorption coefficients at 227.5 and 222 nm were determined for each of the six esters using the experimental apparatus with a 185-cm cell. Laser energies were measured with a Molectron J25 joulemeter and were corrected for window absorption. Sample pressures were varied from 200 to 800 mTorr. Within the limits of experimental uncertainty, the absorption coefficient at a particular wavelength was not dependent on the identity of the ester. The absorption coefficients were found to be 4.5 ($\pm$0.4) $\times$ 10^{-3} and 5.8 ($\pm$0.5) $\times$ 10^{-3} cm^{-1} $Torr^{-1}$ at 227.5 and 222 nm, respectively. These results are consistent with the published ethyl formate spectrum which has absorption coefficients of approximately 4.9 $\times$ 10^{-3} and 6.5 $\times$ 10^{-3} cm^{-1} $Torr^{-1}$ at the corresponding wavelengths.[1]

The continuous wave infrared laser source was a Laser Photonics liquid nitrogen cooled system. For the 227.5-nm experiments, the IR beam was steered into the cell slightly off-axis with the UV beam so that the beams would overlap over the 275 cm path length. Dichroic beam splitters were used to overlap the UV and IR beams during the 222-nm experiments. Identical beam alignment was carefully maintained for all experiments at a given excitation wavelength. The infrared output was directed through a PTI $^1/_4$-m monochromator, which served to filter the detector from stray light and unwanted second mode emission from the IR source. Infrared intensities were monitored with a Judson HgCdTe detector with matched preamplifier. The rise time of the detection system was approximately 1 μs. Transient IR signals were averaged over 1000 UV laser shots using a LeCroy 9410 digital oscillosope and then transferred to a Northgate 386 PC for storage and later analysis.

The 1986 AFGL HITRAN database[16] was used for identification of CO_2 and CO transitions and for calculations of quantum yields of these species. Calibration of the IR laser wavelength in the HCOOH probe region was performed using water vapor as a reference gas, with assignments taken from the HITRAN database. Formic acid transitions were then identified from literature assignments[11] of ν_3 lines. During transient IR measurements, the diode laser was tuned to the peak of a transition for the product molecule of interest. No transient signals were observed with the laser detuned slightly from the probe line. All of the quantum yield experiments were performed using the HCOOH transition ($\nu_3 = 0$, $J = 9_{0,9}$) $\rightarrow$ ($\nu_3 = 1$, $J = 10_{0,10}$) at 1784.023 cm^{-1}.

Reference samples of formic acid (Lancaster, 97%), CO_2 (Airco, 99.9%), and CO (Airco, C. P. Grade) were prepared by degassing prior to use with several freeze−pump−thaw cycles in liquid nitrogen. Commercial samples of ethyl formate (Aldrich, 97%), *n*-propyl formate (Kodak, 99%), isopropyl formate (Pfaltz & Bauer), *n*-butyl formate (Sigma, 97%), isobutyl formate (Aldrich, 97%), and *tert*-butyl formate (Aldrich, 99%) were carefully purified[17] before use to eliminate any residual HCOOH which would interfere with experimental measure-

(11) Weber, W. H.; Maker, P. D. *J. Mol. Spectrosc.* **1987**, *121*, 243.
(12) (a) Gray, P.; Thynne, J. C. J. *Nature* **1961**, *191*, 1357. (b) Thynne, J. C. J. *Trans. Faraday Soc.* **1962**, *58*, 676.
(13) Ausloos, P. *Can. J. Chem.* **1958**, *36*, 383.
(14) Yee Quee, M. J.; Thynne, J. C. J. *Trans. Faraday Soc.* **1967**, *63*, 1656.
(15) (a) Kreutz, T. G.; O'Neill, J. A.; Flynn, G. W. *J. Chem. Phys.* **1987**, *87*, 4598. (b) Holland, J. P.; Rosenfeld, R. N. *J. Chem. Phys.* **1988**, *89*, 7217. (c) Weiner, B. R.; Pasternack, L.; Nelson, H. H.; Prather, K. A.; Rosenfeld, R. N. *J. Phys. Chem.* **1990**, *94*, 4138. (d) Hall, G.; Vanden Bout, D.; Sears, T. J. *J. Chem. Phys.* **1991**, *94*, 4182. (e) Suzuki, T.; Kanamori, H.; Hirota, E. *J. Chem. Phys.* **1991**, *94*, 6607. (f) Alvarez, R. A.; Moore, C. B. *J. Phys. Chem.* **1994**, *98*, 174.
(16) Rothman, L. S.; Gamache, R. R.; Goldman, A.; Brown, L. R.; Toth, R. A.; Pickett, H. M.; Poynter, R. L.; Flaud, J.-M.; Camy-Peyret, C.; Barbe, A.; Husson, N.; Rinslaud, C. P.; Smith, M. A. H. *Appl. Opt.* **1987**, *26*, 4058.
(17) Riddick, J. A.; Bunger, W. B. *Organic Solvents, Physical Properties and Methods of Purification*; Wiley-Interscience: New York, 1970; Vol. 2, pp 748−55.

ments. Each ester sample was washed successively with a saturated NaCl solution and a saturated $NaHCO_3$ solution and then dried for a minimum of 2 h with $MgSO_4$. Following this procedure, samples were distilled at their normal boiling points and finally degassed by several freeze−pump−thaw cycles at liquid nitrogen temperature.

Calculations

Semiempirical calculations were performed using AMPAC.[18] Most calculations were performed using AM1,[19] with some selected comparisons of ethyl formate structures and energies made with MINDO/3.[20] For each of the six formate esters of interest here, heats of formation were obtained for the ground state, first excited singlet state, first excited triplet state, and transition states for hydrogen abstraction on the excited singlet and triplet surfaces. The PRECISE option was used for each optimization. Verification of structures as either minima on the relevent surfaces or as true transition states was made by calculating force constants for the geometry of interest. Minima were found to contain no negative force constants and the transition state structures were found to have exactly one negative force constant. Transition states were located by first calculating geometries on either side of the transition state and then choosing one geometry on each side, close to the presumed transition state, as the reactant and product in a saddle point calculation.[21] Results are given with sufficient numbers of figures to allow for reproduction of the calculations and thus do not necessarily imply the expected degree of accuracy.

Ab initio calculations for selected ethyl formate structures and energies were executed using GAUSSIAN 92, Revision D.3.[22] For most calculations, AM1 results were used for the initial geometry guess and STO-3G optimizations were performed prior to using larger basis sets. For the ethyl formate ground state, restricted Hartree−Fock (RHF) optimizations were performed. MP2 optimizations[23] were also performed for both of the ground state conformers. Unrestricted Hartree−Fock (UHF) calculations were also used to obtain the T_1 structure and then to determine the transition state for triplet state intramolecular hydrogen abstraction. Normal mode calculations were performed for each stationary point, and minima and transition state structures were verified by the presence of respectively zero or one negative eigenvalue in the second derivative matrix. Computational limitations precluded frequency calculations for the MP2 ground states. Single point MP2 calculations were performed in order to estimate the triplet state hydrogen abstraction activation energy. Zero point energies were scaled[24] by 0.89 prior to use in the relative energy calculations. Absolute energies are given in units of Hartree.

Results

A. Product Yields. Production of CO_2 from the photolysis of ethyl formate at 227.5 nm was observed as shown in Figure 1. The transmitted infrared intensity decreases following the UV laser pulse at time $t = 0$ and then increases back to the baseline at longer times. The primary loss mechanism for photoproducts in our experimental configuration is diffusion out of the volume of the IR collection zone. In Figure 1a, the $00^00 \rightarrow 00^01$ P64 transition at 2286.9320 cm^{-1} was monitored. Assuming that the nascent rovibrational populations are relaxed to a room-temperature Boltzmann distribution, an estimate for the CO_2 quantum yield can be obtained using the known UV and IR absorption coefficients. For these estimates, we assume that the effective volume for the overlap of the two lasers is 8.6 cm^3 and that all of the CO_2 molecules are detected prior to diffusing out of the probe volume. The Figure 1a data correspond to a CO_2 quantum yield of 0.5 ± 0.1. The uncertainty reflects experimental fluctuations in sample pressure and laser power as well as uncertainty in determining the effective overlap between the two laser beams. Similar yields are obtained when monitoring other $00^00 \rightarrow 00^01$ transitions for 1- to 3-Torr ethyl formate samples.

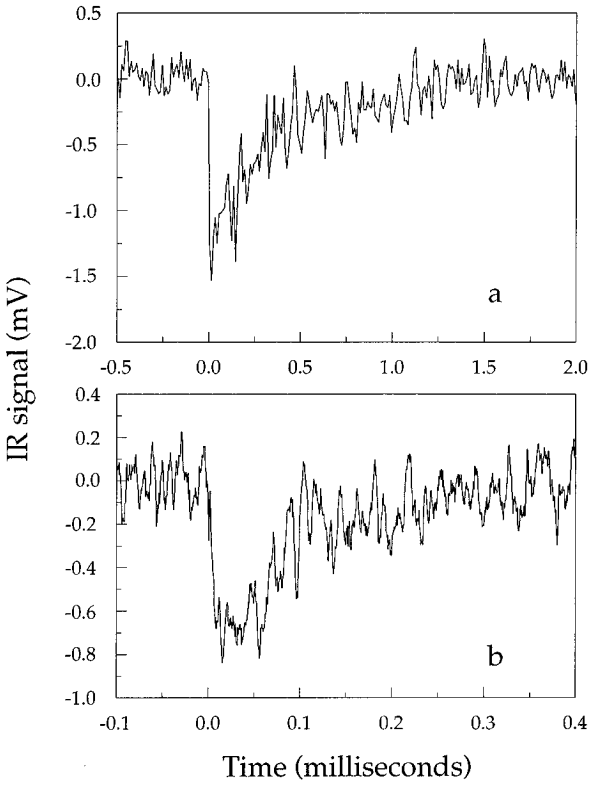

Figure 1. Transient IR detection of CO_2 from ethyl formate. Infrared probe transitions are listed in the text. (a) Typical transient signal from the CO_2 00^00 state. Ethyl formate pressure was 1.1 Torr, infrared $I_0 =$ 1 V, and the UV laser energy was 0.39 mJ/pulse. (b) Typical transient signal from the CO_2 01^10 state. The ethyl formate pressure was 320 mTorr, infrared $I_0 = 0.41$, and the UV laser energy was 0.47 mJ/pulse.

At lower ethyl formate sample pressures, transitions involving higher vibrational states have also been observed. Figure 1b shows the result from a 320-mTorr ethyl formate sample when the CO_2 $01^10 \rightarrow 01^11$ P34f at 2291.4170 cm^{-1} transition was monitored. This particular transition probes molecules with one ^{18}O isotope (natural abundance) which is convenient for minimizing diode laser absorption along the beam path. Weaker transient signals from CO_2 in the 02^20 states have also been obtained using similar experimental conditions. In contrast, negligible CO_2 formation at 227.5 nm was observed in transient IR experiments with the substitution of isobutyl formate for ethyl formate. We estimate that the CO_2 quantum yield was less than 0.1 in this case.

(18) *QCPE Publication 506*; Department of Chemistry, Indiana University, Bloomington, IN 47405.

(19) Dewar, M. J. S.; Zoebisch, E. G.; Healy, E. F.; Stewart, J. J. P. *J. Am. Chem. Soc.* **1985**, *107*, 3902.

(20) Bingham, R. C.; Dewar, M. J. S.; Lo, D. H. *J. Am. Chem. Soc.* **1975**, *97*, 1285.

(21) Dewar, M. J. S.; Healy, E. F.; Stewart, J. J. P. *J. Chem. Soc., Faraday Trans.* **1984**, *80*, 227.

(22) Frisch, M. J.; Trucks, G. W.; Head-Gordon, M.; Gill, P. M. W.; Wong, M. W.; Foresman, J. B.; Johnson, B. G.; Schlegel, H. B.; Robb, M. A.; Replogle, E. S.; Gomperts, R.; Andres, J. L.; Raghavachari, K.; Binkley, J. S.; Gonzalez, C.; Martin, R. L.; Fox, D. J.; Defrees, D. J.; Baker, J.; Stewart, J. J. P.; Pople, J. A.; Gaussian, Inc.: Pittsburgh, PA, 1992.

(23) Møller, C.; Plesset, M. S. *Phys. Rev.* **1934**, *46*, 618.

(24) Pople, J. A.; Schlegel, H. B.; Krishnan, R.; DeFrees, D. J.; Binkley, J. S.; Frisch, M. J.; Whiteside, R. A.; Hout, R. F.; Hehre, W. J. *Int. J. Quantum Chem., Symp.* **1981**, *15*, 269.

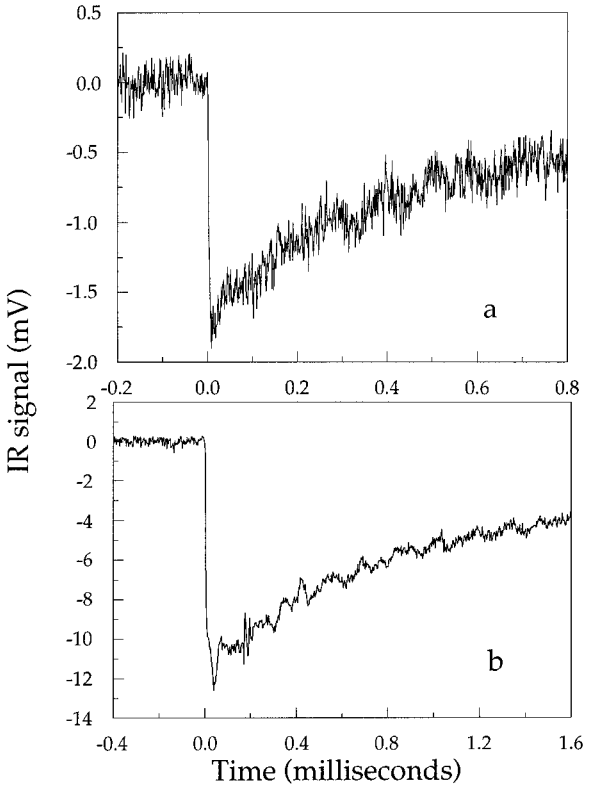

Figure 2. Transient IR detection of HCOOH. The infrared probe transition is described in the text. (a) Signal obtained from 227.5-nm photolysis of a 400-mTorr sample of isobutyl formate with an IR I_0 of 1.7 V and an UV laser energy of 0.35 mJ/pulse. (b) Signal obtained from 222-nm photolysis of a 420-mTorr sample of *tert*-butyl formate with an IR I_0 of 1.0 V and an UV laser energy of 5 mJ/pulse.

No transient absorption was observed for CO at 227.5 nm. Photolysis of static samples of ethyl formate was performed in order to verify that the negative results for CO determination were not due to inadequate quenching of the nascent internal energy distribution since the probe transition involved $v = 0$ CO. Pressures were increased up to 20 Torr and photoproducts were monitored with the diode laser modulation set to scan over an entire mode, typically 2−4 cm^{-1}. Photolyzing static gas samples at repetition rates of 1−10 Hz led to growth of IR lines for HCOOH and CO_2 after several minutes but there was again no evidence for significant CO production at 227.5 nm. We were, however, able to observe CO production at 240 and 237.5 nm. Five-Torr ethyl formate samples were photolyzed at 5 Hz for 40 min. CO quantum yields of 0.02 to 0.03 were calculated from the observed CO IR absorption intensities, assuming that CO occupies the entire 927 cm^3 cell volume at the same pressure as determined in the IR probe volume. The calculated yield represents an upper limit on direct CO formation since secondary reactions are likely when photolyzing static samples for extended periods of time.

Transient HCOOH IR absorption signals were obtained from each ester sample by monitoring changes in transmitted intensity with the diode laser tuned to the $(v_3 = 0, 9_{0,9}) \rightarrow (v_3 = 1, 10_{0,10})$ transition. Typical results are shown in Figure 2a for photolysis at 227.5 nm and Figure 2b for 222-nm excitation. Values for ΔI, the net change in infrared intensity, were obtained by assuming an exponential decay of the absorption and then fitting the decay portion of the transient signal back to time $t = 0$. Relative quantum yields were then determined by normalizing the observed change in IR intensity by the factors which vary during the experiments. The normalization was done using the equation shown below where I_0 is the IR intensity at the peak

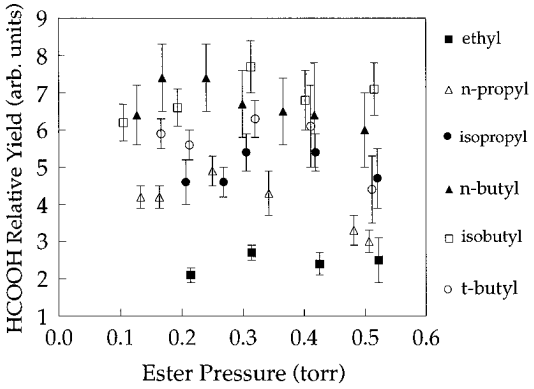

Figure 3. Relative HCOOH yields. Relative quantum yields obtained from 227.5-nm photolysis of formate esters. Error bars are calculated by standard propagation of error and contain contributions from fluctuations in sample pressure, UV laser power, and uncertainty in decay fitting.

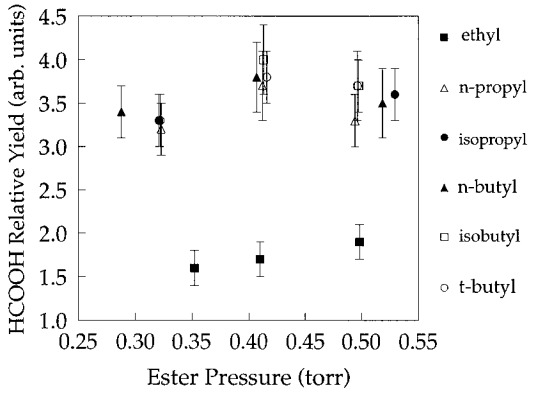

Figure 4. Relative HCOOH yields. Relative quantum yields obtained from 222-nm photolysis of formate esters. Error bars are calculated by standard propagation of error and contain contributions from fluctuations in sample pressure, UV laser power, and uncertainty in decay fitting.

center, p is the ester pressure, and UV is the UV laser energy reading. I_0 readings were determined with the ester sample flowing through the cell at the designated pressure in order to correct for the weak, structureless IR absorption of the esters in this IR wavelength region.

$$\phi_{rel} = \frac{\Delta I/I_0}{UV_\alpha p} \tag{8}$$

Figures 3 and 4 show the results for relative quantum yield determination at a variety of ester pressures. In order to facilitate comparison of molecular structure effects, the average value of the quantum yield for each ester was divided by the number of γ-hydrogen atoms and then normalized to the ethyl formate yield per γ-hydrogen equal to one. These results are listed in Table 1.

B. Computational Results. Table 2 lists the results of AM1 calculations for heats of formation of the ground state ester, designated as S_0, excited triplet, T_1, excited singlet, S_1, transition state for triplet hydrogen abstraction, $T_1^‡$, and the transition state for hydrogen abstraction on S_1, $S_1^‡$. Only the lowest energy conformer found is reported. The AM1 calculations resulted in splittings between the singlet and triplet excited states on the order of 5−6 kcal/mol for each of the six esters. Carbonyl bond lengths were found to be elongated, relative to the ground state, by approximately 0.1 Å in both excited states. The out-of-plane (OOP) distortion around the carbonyl group was found to be 33° in T_1 and 38° in $T_1^‡$. Some of the characteristic structural parameters for the excited states are listed in Table 3.

Table 1. Relative Quantum Yields for HCOOH Production

	227.5 nm		222 nm	
formate ester	rel yield (arb. units)	yield/ γ-H[a]	rel yield (arb. units)	yield/ γ-H[a]
Primary Hydrogen Atom Abstraction				
ethyl	2.4 ± 0.2	1.0	1.7 ± 0.2	1.0
isopropyl	4.9 ± 0.4	1.0	3.5 ± 0.2	1.0
tert-butyl	5.7 ± 0.7	0.8	3.6 ± 0.4	0.7
Secondary Hydrogen Atom Abstraction				
n-propyl	4.0 ± 0.7	2.5	3.4 ± 0.3	3.0
n-butyl	6.7 ± 0.6	4.2	3.6 ± 0.2	3.2
Tertiary Hydrogen Atom Abstraction				
isobutyl	6.9 ± 0.6	8.6	3.8 ± 0.2	6.7

[a] Normalized with respect to the yield/γ-H of ethyl formate.

Table 2. AM1 Results

	stationary points (kcal/mol)					
formate	S_0	lit.[a]	T_1	S_1	$T_1^{\ddagger}$	$S_1^{\ddagger}$
ethyl	−97.0	−92	−21.6	−16.1	−9.92	−5.99
n-propyl	−103	−110	−28.8	−23.1	−17.9	−13.0
isopropyl	−101	−97	−25.1	−20.1	−14.5	−10.3
n-butyl	−110	−103	−35.5	−29.8	−24.7	−20.5
isobutyl	−108	−102	−33.4	−27.5	−22.8	−18.5
tert-butyl	−102	−106	−26.7	−20.2	−16.2	−12.0

[a] References 23 and 24.

Table 3. Ethyl Formate Ground and Excited State Structures

	state	C═O (Å)	energy (hartree)	OOP (deg)	O---H (Å)	H---C (Å)
AM1	S_0	1.229	*a*	0		
	T_1[b]	1.332	*a*	33		
	S_1[b]	1.347	*a*	22		
	$T_1^{\ddagger}$ [b]	1.323	*a*	38	1.384	1.226
	$S_1^{\ddagger}$ [b]	1.328	*a*	33	1.418	1.209
ab initio						
HF/6-31G	S_0[c]	1.208	−266.6976	0		
MP2/6-31G*		1.216	−267.5673	0		
UHF/3-21G	T_1	1.410	−265.2424	49		
UHF/6-31G		1.396	−266.6021	48		
UHF/6-31G*		1.363	−266.7141	50		
UHF/3-21G	$T_1^{\ddagger}$	1.403	−265.1909	48	1.197	1.353
UHF/6-31G		1.394	−266.5460	47	1.208	1.340
UHF/6-31G*		1.361	−266.6595	50	1.214	1.312

[a] See Table 2. [b] Calculated with C. I. = 2. [c] S_0 values determined for the *s-cis,trans conformer*.

Ab initio calculations were performed for the *s-cis,trans* and *s-cis,gauche* conformers of the ethyl formate ground state. Both of these conformers have been observed spectroscopically[25−27] and are similar in energy. At the MP2/6-31G//RHF/6-31G level, the *s-cis,trans* conformer is found to be lower in energy than the *s-cis,gauche* structure by 0.2 kcal/mol. This is in agreement with experimental results,[25,27] which also support the assignment of the *s-cis,trans* conformer as the most stable species.

An unrestricted Hartree−Fock calculation was carried out in order to locate the transition state for hydrogen abstraction on the triplet excited state surface. At the MP2/6-31G//UHF/6-31G level, the activation energy for this process was found to be 14 kcal/mol. Figure 5 illustrates the relative energetics obtained via AM1 and *ab initio* methods.

Select MINDO/3 calculations were also performed. This method was used with and without configuration interaction to calculate excited states and did not lead to the significant

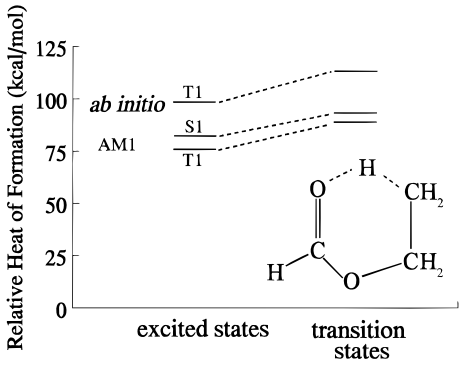

Figure 5. Relative heats of formation. Energy levels are depicted relative to the ethyl formate ground state calculated at the same level of theory. *Ab initio* energies are determined at the MP2/6-31G//HF/6-31 level and corrected for zero-point energy. A representation of the transition state for the triplet hydrogen abstraction channel, as calculated via AM1, is shown below the transition state energy levels. The energy of a 227.5-nm photon corresponds to 125 kcal/mol.

elongation of the carbonyl bond length that is expected for (nπ^*) states. The C═O bond lengths obtained were 1.202, 1.206, and 1.240 Å for S_0, T_1, and S_1, respectively. The splitting between the lowest singlet and triplet excited states was found to be 24 kcal/mol. In addition, the T_1 HCO bond angle of 78° appears distorted when compared with the values of 117° and 111° determined in AM1 and *ab initio* (UHF/6-31G*) calculations, respectively.

Discussion

A. Experimental. Time-resolved infrared absorption monitoring of photoproducts, using the nonperturbing diode laser technique, indicates that CO production from ethyl formate is not an important primary process at 227.5 nm. This precludes reaction channel 3 from being important under moderate pressure gas-phase conditions. Channel 1 was also a potential, although unlikely, source for CO. The barrier for production of CO from HCO is approximately 19 kcal/mol.[28] Depending on choice of HCO and ethyl formate heats of formation, the threshold for secondary production of CO from channel 1 corresponds to 3000[28] to 5000[29] cm^{-1} less than the energy of a photon at 227.5 nm. It is impossible to unambiguously judge the importance of channel 1 without monitoring HCO or CH_3CH_2O. In most examples of Norrish Type I reactivity of asymmetric ketones, the lower energy α-cleavage channel dominates.[1] A similar trend for esters would favor channel 2 over channel 1.

Carbon dioxide formation is a major channel for ethyl formate. This is consistent with the energetics for secondary decomposition of the Norrish Type I product of channel 2. The threshold for the production of CO_2 is 13 000 cm^{-1} less than the photon energy since the barrier for decarboxylation[12] of the radical produced in channel 2 is approximately 1−2 kcal/mol. The competition between channels 2 and 4 is evident when ethyl formate is compared with isobutyl formate. A high yield of HCOOH is correlated with a low yield of CO_2, eliminating the possibility[30] of secondary photolysis or reactions of formic acid as the primary source of CO_2. Additional work is in progress in our laboratory to explore the photodissociation dynamics of the CO_2 channel.

(25) Riveros, J. M.; Wilson, E. B., Jr. *J. Chem. Phys.* **1967**, *46*, 4605.
(26) Kaushik, V. K. *Chem. Phys. Lett.* **1980**, *70*, 317.
(27) Maes, I. I.; Herrebout, W. A.; van der Veken, B. J. *J. Raman Spectrosc.* **1994**, *25*, 679.
(28) Benson, S. W.; O'Neal, H. E. *Kinetic Data on Gas Phase Unimolecular Reactions*; NSRDS-NBS; National Bureau of Standards: Washington, DC, 1970; Vol. 21.
(29) Lias, S. G.; Bartmess, J. E.; Liebman, J. F.; Holmes, J. L.; Levin, R. D.; Mallard, W. G. *J. Phys. Chem. Ref. Data* **1988**, *17*, Suppl. 1.
(30) Singleton, D. L.; Paraskevopoulos, G.; Irwin, R. S. *J. Phys. Chem.* **1990**, *94*, 695.

Comparison of gas-phase HCOOH production from different precursors using a quantum-state-specific probe technique, such as time-resolved infrared diode laser absorption spectroscopy, requires consideration of potential differences in product state distributions. At lower sample pressures and short times, nonstatistical rotational state distributions are observed as discussed in an accompanying communication.[31] Since the nascent internal energy partitioning and translational energy release into HCOOH may not be the same for each of the esters, quantum yield measurements must be performed on equilibrated samples. Working with moderate pressure samples serves to provide adequate collisional equilibration since no clear pressure dependence of the yields is observed. Determining ΔI via fitting the decay portion of the transient signals back to time $t = 0$ allows for analysis of equilibrated samples as well as correction for differences in sample concentrations in the probe volume due to HCOOH diffusion.

The general comparison of molecular structure on the relative Norrish Type II elimination yields remains the same at the two photolysis wavelengths. In each case, production of HCOOH is significantly lower from ethyl formate than from the other esters. At 222 nm, the relative HCOOH yields from the other five esters are all the same, within experimental uncertainty. At the lower photolysis energy there is a somewhat wider range of HCOOH yields. Due to differences in beam geometries, quantitative comparisons of absolute yields at the two wavelengths are not warranted. Normalization of the quantum yields by the number of γ-hydrogens results in clear reactivity trends which depend upon the degree of substitution at the γ-carbon atom.

The pioneering work on formate ester photochemistry was performed by Ausloos.[13,32] Gas- or solution-phase photolysis using a medium-pressure Hanovia lamp was followed by fractional condensation and combustion or mass spectrometric analysis.[32] In the gas-phase experiments on ethyl formate, CO production was found to be higher than CO_2 production. This is in marked contrast to the results obtained in this study where CO production from the molecular elimination channel 3 or from decomposition of the formyl radical produced in channel 1 is negligible. Experiments on methyl formate led to the proposal that CO production was most likely due to secondary reactions,[14] which is consistent with our results. The Type II yields for formate esters determined by Ausloos appeared strongly solvent dependent.[32] In solution, at 303−304 K, propene production from n-propyl formate was observed to be nearly double that of ethene production from ethyl formate.[13,32] Butene formation from n-butyl formate was reported to be comparable to the Type II process in ethyl formate.[13] Gas-phase experiments were reported for ethyl formate and the Type II yields were observed to be temperature independent,[13] consistent with gas-phase studies of the Norrish Type II process of 2-pentanone.[33] We observe a similar trend in the relative yields of HCOOH from ethyl and *n*-propyl formate but find a significantly higher yield from *n*-butyl formate when compared to the solution-phase results.

Most work on structure−activity relationships for Norrish Type II reactivity in aliphatic carbonyls has been carried out in solution. Observed quantum yields reflect the competition between possible decay channels at various stages along the reaction path.[34] In the case of aliphatic carbonyls, there is also experimental evidence for the contribution of both singlet and triplet channels in the final Norrish Type II product yields. The relative contribution of the singlet channel is believed to be dependent upon the type of γ-hydrogen atom being abstracted.[35,36] For the ketone series 2-pentanone, hexan-2-one, and 5-methylhexan-2-one, the relative contributions of triplet and singlet channels vary from nearly all triplet for abstraction of a primary hydrogen to 1:2 singlet−triplet for the secondary hydrogen atom abstraction and equal contributions for the case of tertiary contributions.[37]

The relative quantum yields determined here exhibit a trend which is consistent with the relative reactivity of the hydrogen atoms when normalized with respect to the number of abstractable hydrogens. The effect is not as significant as the differences in intramolecular hydrogen abstraction rates determined for ketones[34] but does follow the same general trend. This is not surprising since the product yields are influenced by the competition at several points along the reaction path.[34] It is interesting to note that the results of reference 11b for Norrish Type II quantum yields lead to similar reactivity trends when normalized with respect to the number of abstractable hydrogen atoms. The normalized yields, scaled to have the yield/γ-H equal to one for the n-propyl ketone, are found to be 0.7 for abstraction of primary hydrogen atoms in the isobutyl case and 3.5 for the abstraction of secondary hydrogen atoms from the n-butyl ketone.

The role of environment in influencing relative contributions of competing decay channels is clearly important. While solvent effects are not an issue in these moderate-pressure gas-phase experiments, there is some collisional interaction on the time scale of the experimental measurements which may influence the competition between different channels. Trapping studies performed on 2-pentanone suggest that the gas-phase triplet diradical lifetime could be on the order of microseconds.[33] Systematic experiments performed in a collision-free environment would be additionally useful in understanding the primary contributions to quantum yields in these systems.

Pressure effects on observed quantum yields are negligible over the pressure range utilized in these studies. This is similar to the results obtained for 2-pentanone.[33] Decreasing HCOOH transient IR absorption signals are observed in our apparatus when the ester pressures are increased to ≥ 1 Torr. Pressure broadening of the HCOOH infrared absorption line used in the probe[38] is responsible for at least some of the apparent decrease in yield. Such effects appear to be negligible in the narrow pressure range used here. The small variation in photolysis wavelength from 227.5 to 222 nm does not influence the relative Type II reactivity of this series of formate esters.

B. Computational. The apparent correlation between the normalized HCOOH yields and the relative reactivity of the γ-hydrogen atoms provided the motivation for computational studies of the hydrogen abstraction step. Semiempirical approaches are attractive for making comparisons among the series of formate esters from the point of view of required computational resources. Previous semiempirical and *ab initio* work on butanal and 2-pentanone has demonstrated that, with proper selection of method, semiempirical approaches provide reasonable estimates for the geometry and activation enthalpy for the triplet state hydrogen abstraction step.[7] While AM1 has been

(31) Niu, Y.; Christophy, E.; Hossenlopp, J. M. *J. Am. Chem. Soc.* **1996**, *118*, 4188.

(32) Ausloos, P. *J. Am. Chem. Soc.* **1958**, *80*, 1310.

(33) O'Neal, H. E.; Miller, R. G.; Gunderson, E. *J. Am. Chem. Soc.* **1974**, *96*, 3351.

(34) Wagner, P. J. In *Rearrangements in Ground and Excited States*; de Mayo, P., Ed.; Academic Press: New York, 1980; pp 381−444.

(35) Turro, N. J. *Modern Molecular Photochemistry*; Benjamin/Cummings: Menlo Park, CA, 1978; pp 386−392.

(36) Horspool, W.; Armesto, D. *Organic Photochemistry: A Comprehensive Treatment*; Ellis Horwood: New York, 1992; pp 195−197.

(37) (a) Yang, N. C.; Elliot, S. P.; Kim, B. *J. Am. Chem. Soc.* **1969**, *91*, 7551. (b) Wilson, R. M. *Org. Photochem.* **1985**, *7*, 339.

(38) Liu, J. M.S. Thesis, Marquette University, 1994.

parametrized for hydrogen bonding, which could possibly be an advantage for hydrogen abstraction transition state modeling, MINDO/3 has been found[7] to provide the best agreement with *ab initio* and experimental excited state geometries for butanal and 2-pentanone.

MINDO/3 does not appear to provide a reasonable estimate of ethyl formate excited state properties. The S_1-T_1 splitting was found to be 24 kcal/mol, significantly higher than expected.[35] The C═O bond lengths did not change, relative to the ground state, in T_1 and increases by only 0.04 Å in S_1. While out-of-plane distortion about the carbonyl group was observed in T_1 in the MINDO/3 calculations, there was a severe distortion of the HCO angle which does not appear reasonable. Calculations were also performed without the use of any C.I. to further test the MINDO/3 approach for ethyl formate. The UHF optimization of T_1 without any configuration interaction lowers the heat of formation by 6.5 kcal/mol. The transition states for hydrogen abstraction on the T_1 were also calculated using MINDO/3 and the barriers for hydrogen abstraction were found to be 20 kcal/mol without any inclusion of C.I. and 24 kcal/mol using the same levels of configuration interaction as were included in the AM1 calculation.

Ab initio calculations were performed for comparison with the AM1 results. The MP2/6-31G optimized ground state geometries were found to be in good agreement with reported rotational constants[25−27] for both the *s-cis,trans* and *s-cis,gauche* conformers. The C═O bond length at the RHF/6-31G level is closer to the experimental value of 1.200 Å for esters.[39] For the calculation of T_1, the characteristic[7] out-of-plane (OOP) distortion and lengthened C═O bonds are observed with both methods. The results listed in Table 3 for the *ab initio* transition state C−H and O−H bond lengths and the OHC bond angle are quite similar to those obtained for butanal in a similar calculation.[6] In the case of butanal, it has been shown that there is a shift toward an "earlier" transition state when the basis set is expanded to include polarization functions and electron correlation at the MP2 level.[7] We observe a similar trend in position of the transition state when using the smaller basis sets. The transition state C−H bond length is 26% longer than that of the other two primary C−H bonds at the 3-21G level. This decreases to 24% at the 6-31G level and 22% at the 6-31G* level, showing a shift to an earlier transition state. The transition state O−H bond length can be compared to the diradical value of 0.9519 Å calculated at the same level of theory[40] and shows a comparable increase in length, i.e. shift to an earlier transition state, as a function of increasing basis set size.

Our AM1 calculations predict a much earlier transition state than is observed with small basis set *ab initio* calculations. The AM1 transition state bond lengths and activation barrier resemble those found for butanal.[6] These results suggest that AM1 is a good choice for comparing the hydrogen abstraction process for the entire series of esters. The ground state enthalpies of formation for each compound were found to be within 4−7 kcal/mol of experimental values.[28,29] The calculated S_0 C═O bond length, 1.23 Å, is slightly longer than the experimentally determined value.[39] The excited state energies are quite low when compared to the observed onset of absorption[1] which corresponds to 112 kcal/mol. Semiempirical approaches, which are parametrized for the ground state, cannot be expected to provide accurate excited state energies. The excited state singlet−triplet splittings calculated here are, however, consistent with experimental observations for other carbonyl compounds.[35] Lengthening of the carbonyl bond by approximately 0.1 Å is observed for both the singlet and triplet state as is expected for the ($n\pi^*$) transitions of carbonyls.[41] Out-of-plane distortion around the carbonyl group of the triplet excited state is approximately 30°, similar to experimental results for alkanones.[42]

Enthalpies of activation for the hydrogen abstraction step, $\Delta H^{\ddagger} \equiv T_1^{\ddagger}(S_1^{\ddagger}) - T_1(S_1)$, range from 8 to 12 kcal/mol which is reasonable[3] for this type of reaction. Differences between the six molecules are insignificant given the average uncertainties for calculations based on any of the parametrizations in semiempirical models, particularly for the case of an excited state reaction. In analogy with alkanones[35−37] and consistent with quenching experiments,[1] the triplet state reaction may be expected to be the major route for the abstraction of primary hydrogen atoms. Experimental evidence suggests that the difference in activation energy for primary versus secondary hydrogen abstraction is on the order of 1 kcal/mol for ketones.[10b] This is a small difference compared with the expected accuracy of semiempirical approaches, particularly when applied to excited state reactions. The triplet state barrier for hydrogen abstraction from ethyl formate, where the Norrish Type I reaction appears competitive with the Norrish Type II process, is higher than that which is calculated for each of the other formate esters, but more extensive work needs to be done in order to properly characterize the potential surfaces for these systems.

There are other possible reaction channels available for the singlet diradical which can compete with the Norrish Type II elimination. The singlet and triplet diradicals, elimination transition states, the cyclization product, and the carbene formed by abstraction of the formyl hydrogen have been calculated[40] and work is currently in progress to determine the transition state energies for the competing reactions.

Conclusions

Time-resolved infrared diode laser absorption spectroscopy has been utilized to determine relative yields of the Norrish Type II elimination product, HCOOH, from a series of alkyl formate esters. Relative yields are dependent on the nature of the γ-hydrogen atom. The normalized trends in reactivity are 1:3:9 and 1:3:7 for abstraction of primary, secondary, and tertiary hydrogen atoms at 227.5 and 222 nm, respectively. Photolysis of ethyl formate at 227.5 nm results in formation of CO_2, with an estimated quantum yield of 0.5, but no evidence for CO production is observed. AM1 calculations of the hydrogen abstraction step lead to activation enthalpies of 8−12 kcal/mol with an "early" transition state.

Acknowledgment. Support for this work is provided by the National Science Foundation (CHE-9313944). We also acknowledge the Laser Science Topical Group of the American Physical Society for undergraduate summer fellowship support (P.J.P.). We thank Julie A. Mueller and Terrance R. Viegut for help with preliminary studies of CO and CO_2 formation.

JA952532Z

(39) Harmony, M. D.; Laurie, V. W.; Kuczkkowski, R. L.; Schwendeman, R. H.; Ramsay, D. A.; Lovas, F. J.; Lafferty, W. J.; Maki, A. G. *J. Phys. Chem. Ref. Data* **1979**, *8*, 619.

(40) Christophy, E.; Hossenlopp, J. M. Unpublished results.

(41) Hadad, C. M.; Foresman, J. B.; Wiberg, K. B. *J. Phys. Chem.* **1993**, *97*, 4293.

(42) Tominaga, K.; Yamauchi, S.; Hirota, N. *J. Phys. Chem.* **1990**, *94*, 4425.